Electronic Supplementary Material (ESI) for Journal of Materials Chemistry C.

$AlCl_3$-promoted growth of alkylated carbon dots with enhanced nonlinear optical response

Dandan Lu,[a] Keyang Yin,[a] Shida Hou,[a,b] Penghui Li,[a,b] Hongxia Zhu,[c] Hongguang Li,[a,*] Jingcheng Hao[a]

[a] *Key Laboratory of Colloid and Interface Chemistry, Ministry of Education, School of Chemistry and Chemical Engineering, Shandong University, Jinan 250100, Shandong, China*

[b] *China Research Institute of Daily Chemistry Co., Ltd, Taiyuan 030001, China.*

[c] *State Key Laboratory of Biobased Materials and Green Papermaking, Qilu University of Technology (Shandong Academy of Science), Jinan 25035, China*

* Author to whom correspondence should be addressed, E-mail: hgli@sdu.edu.cn

1. Experimental details

1.1 Materials and methods

Dodecylamine (DDA, 98%), *o*-dichlorobenzene (ODB, analytical grade), anhydrous aluminum chloride ($AlCl_3$, 99%) and anhydrous ferric chloride ($FeCl_3$, 99%) were purchased from Aladdin Biochemical Technology Co., Ltd (Shanghai, China). Polymethylmethacrylate (PMMA, average Mw: ~350000) was purchased from Sigma-Aldrich. Ethanol, dichloromethane (CH_2Cl_2), *n*-hexane and N,N-dimethylformamide (DMF) were obtained from local supplier with the quality of analytical grade. All chemicals were used without further purification. Glasswares, including 60 mm glass petri dishes were also obtained from local supplier.

Fourier transform infrared (FTIR) spectra were recorded on a spectrometer (Tensor II) using KBr pellets. High-resolution transmission electron microscopy (HRTEM) images of CDs were recorded on a JEM2100 instrument operating at 200 kV. For sample preparation, a drop of sample solution (~20 μL, in *n*-hexane) was placed on a holey-carbon coated copper grid (300 meshes) and dried by an infrared lamp. X-Ray photoelectron spectroscopy (XPS) spectra were recorded on an X-ray photoelectron spectrometer (ESCALAB 250) with a monochromatized Al Kα X-ray source (1486.71 eV). Atomic force microscopy (AFM) observation was carried out on a Dimension ICON3 scanning probe microscope (Bruker AXS S.A.S.) in tapping mode in air under ambient conditions using iron disc as substrate. Raman spectra were obtained from a confocal microscopic Raman spectrometer (Lab Ram HR Evolution) equipped with a 325 nm laser with a total power of 25-30 mW. In our measurement, the power was set at 50% of the total power, and the time for data collection is 10 s. UV-vis measurements of the CDs solution were carried out on a UV-vis-NIR spectrometer (cary 5000). Fluorescence spectra were obtained by a spectrofluorometer (FluoroMax-4). The absolute

fluorescence quantum yield (Φ) and fluorescence lifetime (τ) were measured with a spectrofluorometer (FLSP920, Edinburgh Instruments LTD). For measurement of Φ, the CDs were dissolved in DMF. For other measurements, the CDs were dissolved in ethanol.

1.2 Synthesis of CDs

The alkylated, N, Al co-doped CDs (*a*-Al-CDs) were synthesized following the procedures developed by us recently. [1,2] In brief, 9.26 g DDA and 6.2 g $AlCl_3$ were added to 50 mL ODB. The mixture solution was transferred to a 100 mL three-necked flask for pyrolysis at 140 °C for 48 h. After that, the mixture was naturally cooled to room temperature and purified by silica gel chromatography using *n*-hexane as an eluent to remove ODB first and then ethanol to get *a*-Al-CDs. Ethanol was removed under reduced pressure and the crude product was further dried in vacuum. CDs without Al-doping (*a*-CDs) was obtained by the same way in the absence of $AlCl_3$.

1.3 Preparation of CDs/PMMA composite films

The CDs/PMMA composite films were prepared by a simple volatilization method. In a typical experiment, 85.7 mg PMMA was added to 2 mL of CH_2Cl_2. The mixture was sonicated for 30 min to aid the total dissolution of PMMA. To this CH_2Cl_2 solution of PMMA was added desired amounts of CDs which was pre-dissolved in 1 mL CH_2Cl_2. The mixed solution was sonicated for 10 min before being poured into a glass petri dish with a diameter of 60 mm. The sample was then kept at room temperature for 24 h for solvent evaporation. For *a*-Al-CDs/PMMA composite films, amounts of added *a*-Al-CDs was varied to be 0.43 mg, 0.86 mg, 2.14 mg, 3.10 mg and 4.5 mg, which corresponds to an *a*-Al-CDs content of 0.5 wt%, 1.0 wt%, 2.5 wt%, 3.5 wt% and 5.0 wt%, respectively. For comparison, composite film containing 0.43 mg of *a*-CDs was also prepared using the same strategy.

1.4 Evaluation of NLO properties

Third-order NLO absorption of the composite films was evaluated using the open-aperture *Z*-scan technique (Beamtech Optronics Co., Ltd.). A Q-switched Nd: YAG 532 nm laser with a pulse width of 5 ns and a repetition rate of 10 Hz was used as the light source. The laser pulses were focused onto the film using a converging lens and the sample was moved from -*z* to +*z*, where z = 0 represents the focal point and the data were collected using a dual-channel power meter that was interfaced with a computer using LabVIEW software. The nonlinear absorption coefficient is calculated from the intensity dependent transmittance (*T*), which was measured as a function of *z*. The pulse repetition rate was 10 Hz and the beam waist at focus was calculated to be 18 μm. Each measurement was performed at least twice to ensure the reproducibility of the data. The method to obtain values of nonlinear absorption coefficient β could be found elsewhere.[1]

2. Additional data

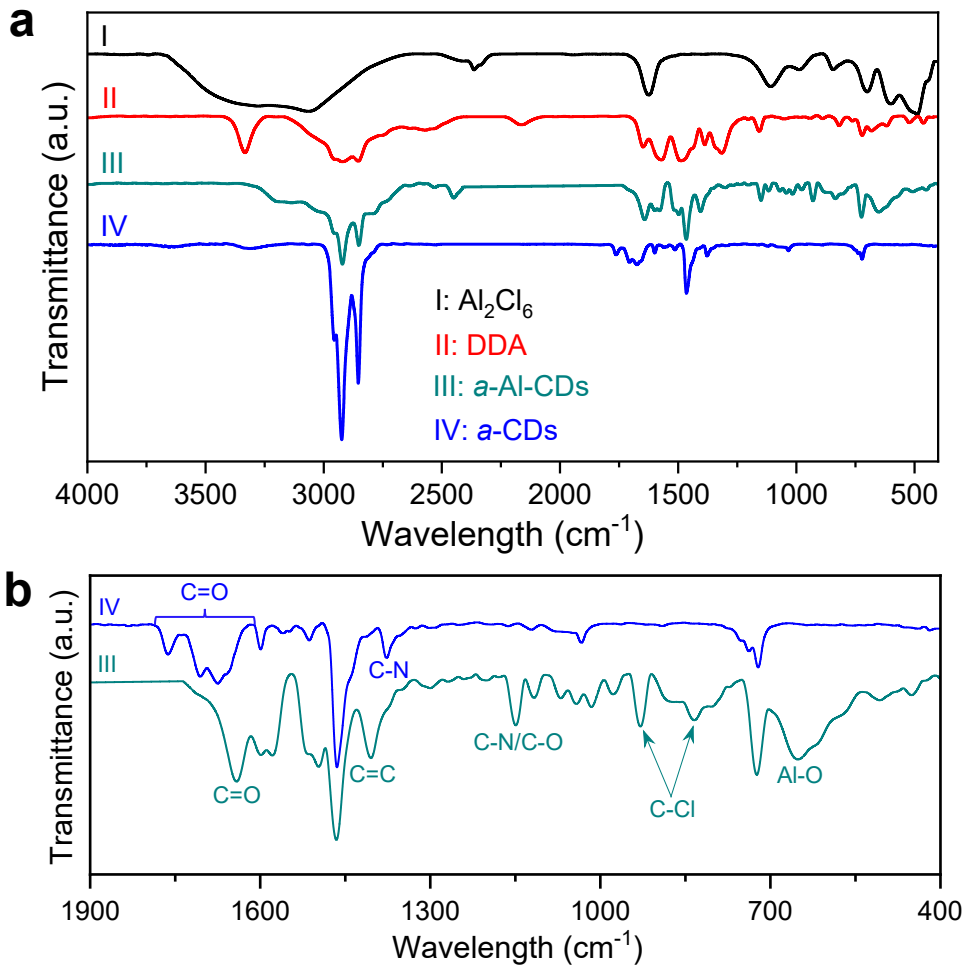

Fig. S1 a) FTIR spectra of *a*-Al-CDs and *a*-CDs recorded between 4000 and 400 cm^{-1}. The results from DDA and $AlCl_3$ are also included for comparison. b) Enlarged spectra between 1900 and 400 cm^{-1} for *a*-Al-CDs and *a*-CDs, with interested peaks assigned.

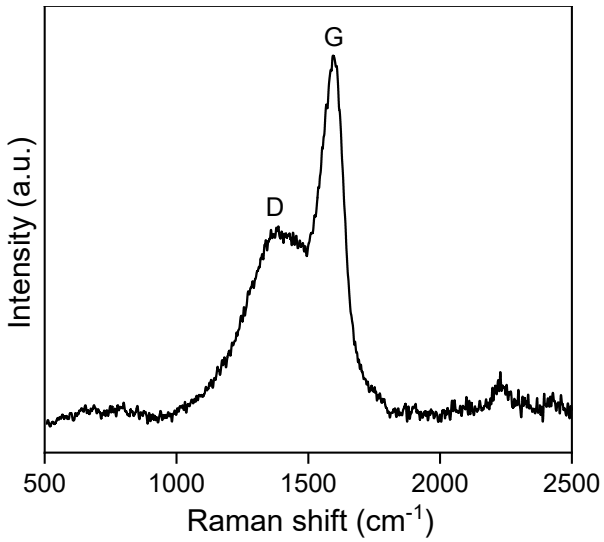

Fig. S2 Raman spectra of *a*-Al-CDs.

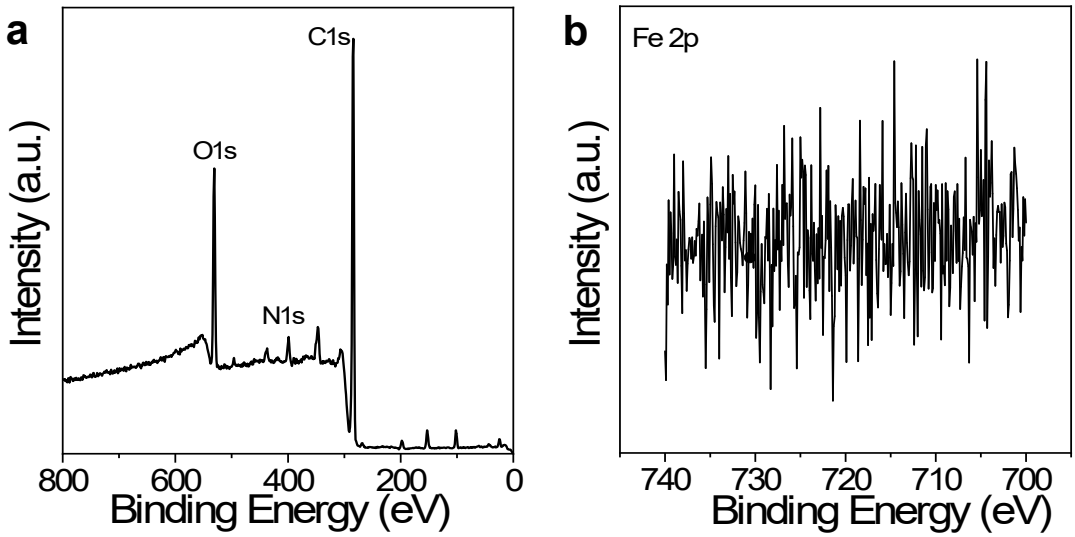

Fig. S3 Full-range survey (a) and high-resolution Fe2p spectrum (b) of CDs prepared by pyrolyzing DDA in *o*-dichlorobenzene at the presence of anhydrous $FeCl_3$. Before measurements, the CDs have been purified by a standard silica gel chromatography following the procedures used for *a*-Al-CDs.

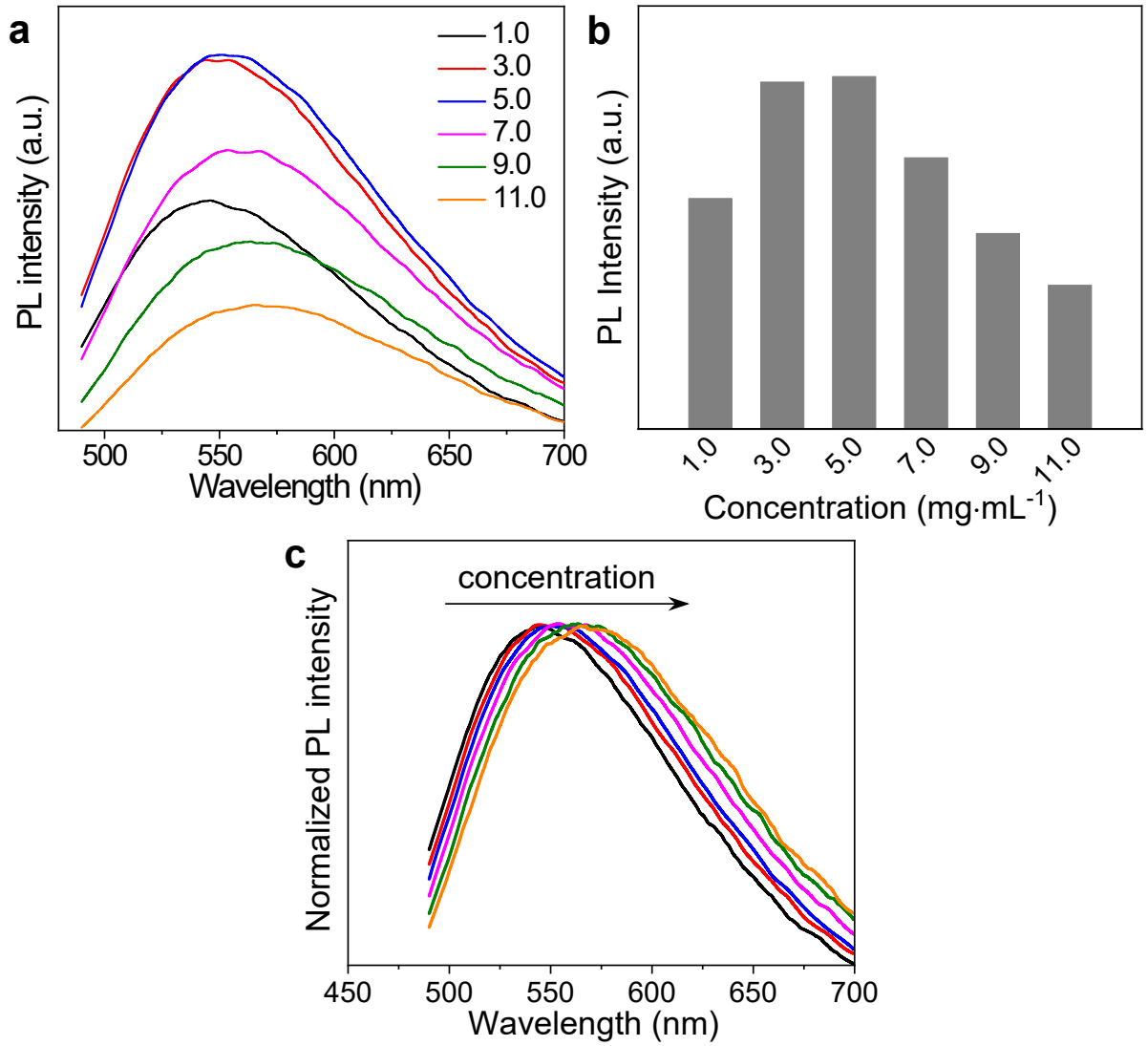

Fig. S4 The concentration-dependent emission of *a*-Al-CDs. a) Emission curve at λ_{ex} = 470 nm as a function of the concentration of CDs indicated inset (mg·mL^{-1}, in ethanol). b) Statistics of the PL intensity as a function of the concentration of CDs. c) Normalized PL intensity of the same series of samples, which highlights the red shift of the emission with increasing concentration of CDs.

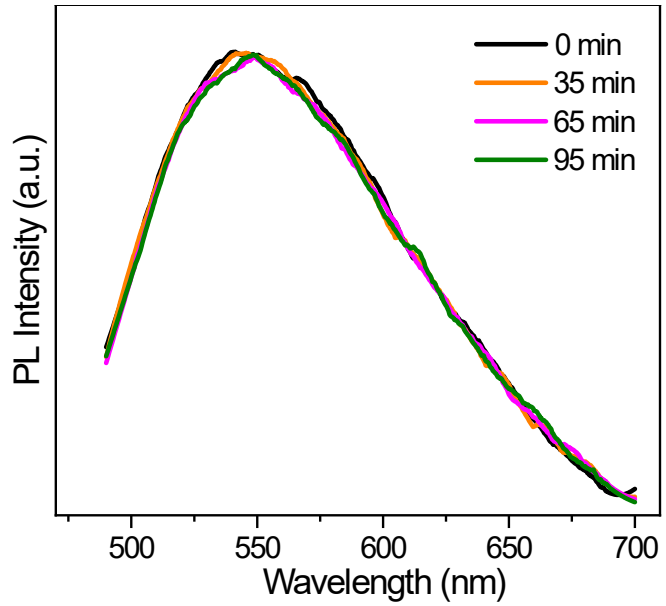

Fig. S5 Emission of *a*-Al-CDs (3.0 mg·mL^{-1} in ethanol) at λ_{ex} = 470 nm under 365 nm UV irradiation for different time as indicated inset.

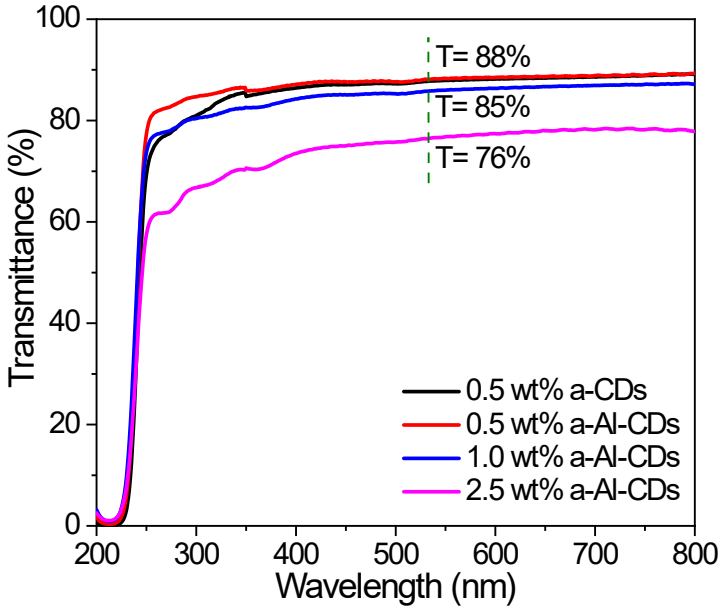

Fig. S6 Emission of *a*-Al-CDs (5.0 mg·mL^{-1} in ethanol) at λ_{ex} = 470 nm under 365 nm UV irradiation for different time as indicated inset.

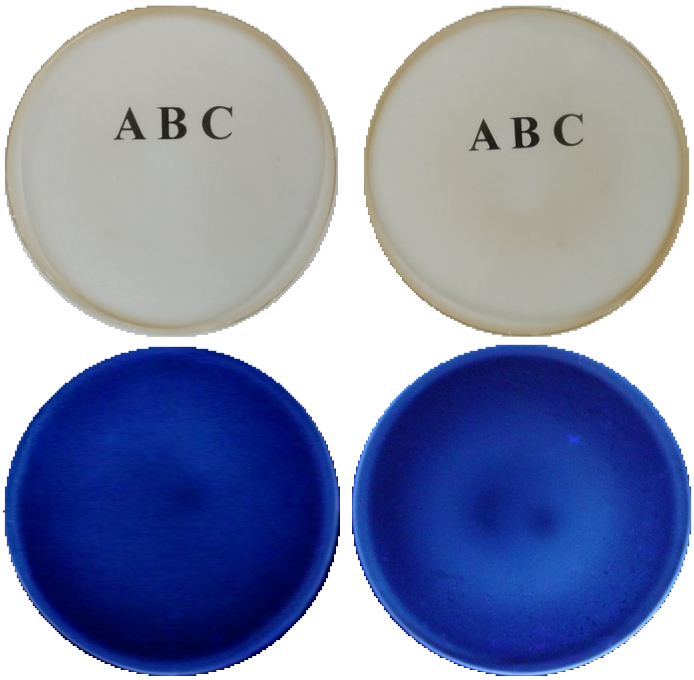

Fig. S7 Photos of the PMMA-based composite films containing 3.5 wt% (left) and 5.0 wt% (right) *a*-Al-CDs, taken under room light (top) and 365 nm UV irradiation (bottom), respectively. Macroscopic phase separation is visible by naked eyes.

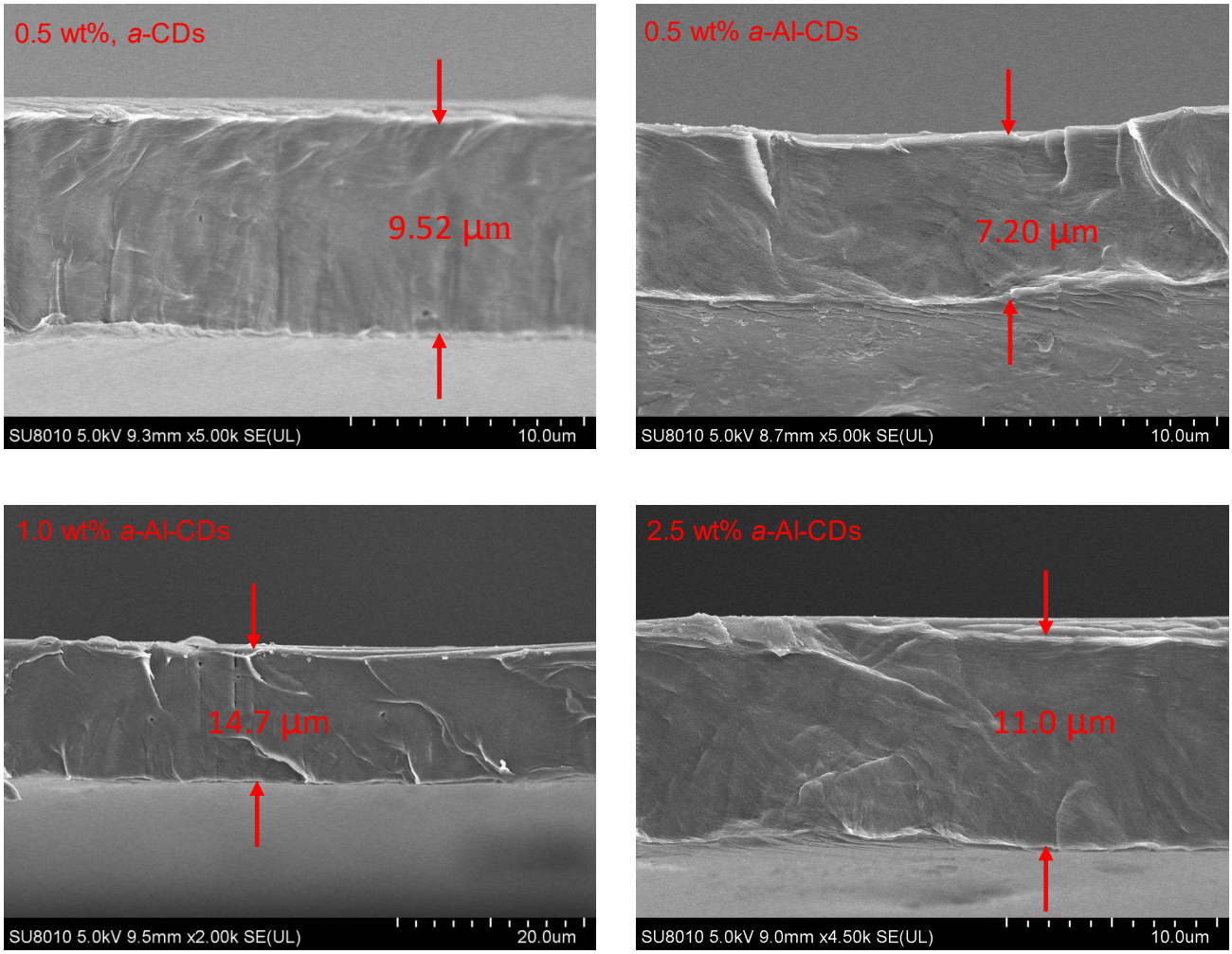

Fig. S8 SEM images on the fracture surfaces of the four PMMA-based composite films loaded with *a*-CDs or *a*-Al-CDs. The thickness of each film is also shown.

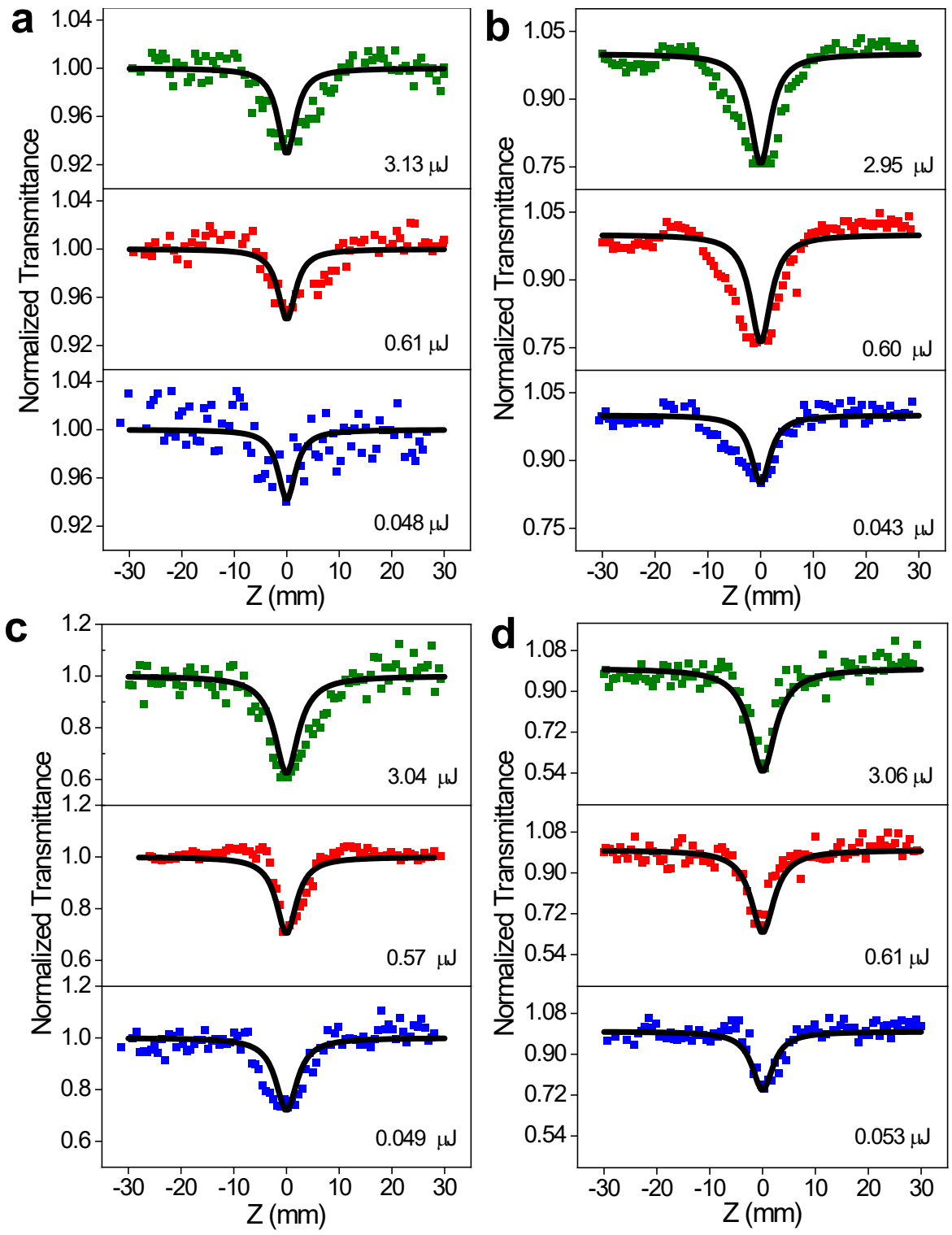

Fig. S9 Normalized transmittance obtained from open-aperture Z-scan at different energy inputs of the laser for four PMMA-based films containing 0.5 wt% *a*-CDs (a) and 0.5 wt% (b), 1.0 wt% (c), 2.5 wt% (d) *a*-Al-CDs, respectively.

3. Tables

Table S1. Results of XPS and elemental analysis (EA) of *a*-CDs and *a*-Al-CDs.

		Al (%)	N (%)	C (%)	O (%)	Cl (%)	H (%)
a-CDs	XPS	\	4.26	64.61	31.13	\	\
	EA	\	3.23	78.77	5.29	\	12.39
a-Al-CDs	XPS	2.52	5.02	80.85	5.79	5.83	\
	EA	\	4.79	55.96	28.22	\	10.81

\: Not present or unavailable by this method.

Table S2. Lifetimes from time-resolved fluorescence study, fluorescence quantum yield (Φ), sizes from TEM observations and the wavelength at which maximum emission occurs in steady-state fluorescence measurements (λ_{em}) for *a*-CDs and *a*-Al-CDs.

Methods		*a*-CDs	*a*-Al-CDs
Decay life	τ_1 (ns)	2.71 (48.81%)	3.08 (59.46%)
	τ_2 (ns)	9.19 (51.19%)	9.57 (40.54%)
	$<\tau>$ (ns)	6.04	5.72
QY (%)		14.13	5.92
Size (nm)		2.62	4.61
λ_{em} (nm)		480	552

Table S3. Nonlinear absorption coefficient (β) for different CDs/PMMA composite films. The thickness of each film obtained from SEM observations (L) and the energies of the laser used in open-aperture Z-scan (E) are also included.

Sample	L (μm)	E (μJ)	β (m/W)
0.5 wt% a-CDs	9.52	0.048	1.4×10^{-6}
		0.61	8.8×10^{-8}
		3.13	2.1×10^{-8}
0.5 wt% a-Al-CDs	7.20	0.043	6.5×10^{-6}
		0.6	7.0×10^{-7}
		2.95	1.5×10^{-7}
1.0 wt% a-Al-CDs	14.7	0.049	6.8×10^{-6}
		0.57	5.3×10^{-7}
		3.04	1.7×10^{-7}
2.5 wt% a-Al-CDs	11.0	0.053	7.0×10^{-6}
		0.61	1.0×10^{-6}
		3.06	3.1×10^{-7}

Table S4. Comparison of the nonlinear optical parameters obtained in current work with previously reported values.

Materials	Experimental details	Nonlinear optical coefficient β	Issuing time	ref
CDs (from lauryl gallate), chloroform	532 nm, 4 ns, 10 Hz (saturable absorption)	-1.4×10^{-9} m/W	2013	3
Hydrophilic CDs (from gallic acid), chloroform	532 nm, 4 ns, 1-10 Hz (saturable absorption)	-1.4×10^{-9} m/W	2014	4
B-doped CDs (from citric acid, boric acid and urea), distilled water	532 nm, 4 ns, 10 Hz (reverse saturable absorption)	5.1×10^{-11} m/W	2015	5
N-doped CDs (from Anhydrous citric acid, silane coupling agent), ethanol	532 nm, 190 fs, (saturable absorption)	-4.8×10^{-13} m/W	2016	6
CDs (from chitin, titania), distilled water	400 nm, 85 fs, (reverse saturable absorption)	8.8×10^{-14} m/W	2016	7
CDs (from graphite rods), distilled water	532 nm, 4 ns, 10 Hz (reverse saturable absorption)	4.1×10^{-10} m/W	2016	8
CDs/MOF (from glucose), MOF complex film	532 nm, 4 ns, 1 Hz (reverse saturable absorption)	1.6×10^{-11} m/W	2017	9
N, Si-doped CDs (from p-phenylenediamine, n-propyl isocyanate, silane coupling agent), silica gel glasses	532 nm, 7 ns, 10 Hz (reverse saturable absorption)	4.21×10^{-10} m/W	2018	10
(CDs)/graphene oxide (GO) (from heparin sodium), aqueous	532 nm, 4 ns, 1 Hz (two photon absorption,	1.59×10^{-13} m/W	2018	11

	nonlinear scattering)			
(CDs)/graphene oxide (GO) (from graphite rod), silica gel glasses	532 nm, 4 ns, 1 Hz (nonlinear absorption, nonlinear scattering)	9.0×10^{-11} m/W	2018	12
N-doped CDs (from 2,3-Diaminophenazine, urea), aqueous solution	532 nm, 21 ps, 10 Hz (saturable absorption to reverse saturable absorption)	4.0×10^{-13} m/W	2019	13
CDs (orange waste peels, citric acid), ethylene glycol	532 nm (reverse saturable absorption)	2.15×10^{-6} m/W	2019	14
CDs/nematic liquid crystal (from ammonium citrate salt), liquid crystal	532 nm, 7 ns, 10 Hz (reverse saturable absorption)	3×10^{-8} m/W	2020	15
N-doped CDs (from aliphatic amine), pure films	1064 nm, 1.5 ps (reverse saturable absorption)	2.73×10^{-2} m/W	2020	1
N-doped CDs (from 2-aminopyrimidine-5-boronic acid), silica films	800 nm, 30 fs (reverse saturable absorption)	4.94×10^{-10} m/W	2020	16
N-doped CDs (from sugarcane bagasse pulp), deionized water	532 nm (reverse saturable absorption)	2.51×10^{-6} m/W	2020	17
B-doped CDs (from activated carbon), n-heptane	442 nm (reverse saturable absorption)	1.49×10^{-6} m/W	2021	18
a-Al-CDs (from aliphatic amine), PMMA films	532 nm, 4 ns, 10 Hz (reverse saturable absorption)	7.0×10^{-6} m/W		Current work

References

1. K. Yin, D. Lu, W. Tian, R. Zhang, H. Yu, E. Gorecka, D. Pociecha, N. Godbert, J. Hao, H. Li, *J. Mater. Chem. C* 2020, **8**, 8980-8991.

2. D. Lu, K. Yin, Y. Zhao, Z. Gao, N. Godbert, H. Li, H. Li, J. Hao, *Colloids Surf., A* 2021, **613**, 126129-126136.

3. A. B. Bourlinos, M. A. Karakassides, A. Kouloumpis, D. Gournis, A. Bakandritsos, I. Papagiannouli, P. Aloukos, S. Couris, K. Hola, R. Zboril, M. Krysmann, E. P. Giannelis, *Carbon* 2013, **61**, 640-643.

4. P. Aloukos, I. Papagiannouli, A. B. Bourlinos, R. Zboril, S. Couris, *Opt. Express* 2014, **22**, 12013-12028.

5. A. B. Bourlinos, G. Trivizas, M. A. Karakassides, M. Baikousi, A. Kouloumpis, D. Gournis, A. Bakandritsos, K. Hola, O. Kozak, R. Zboril, I. Papagiannouli, P. Aloukos, S. Couris, *Carbon* 2015, **83**, 173-179.

6. L. Ma, W. Xiang, H. Gao, J. Wang, Y. Ni, X. Liang, *Dyes Pigment.* 2016, **128**, 1-7.

7. Y. N. Kulchin, A. Y. Mayor, D. Y. Proschenko, I. V. Postnova, Yu. A. Shchipunov, *Quantum Electron.* 2016, **46**, 335-337.

8. L. Bai, S. Qiao, Y. Fang, J. Tian, J. Mcleod, Y. Song, H. Huang, Y. Liu, Z. Kang, *J. Mater. Chem. C* 2016, **4**, 8490-8495.

9. Z. Gu, D. Li, C. Zheng, Y. Kang, C. Wöll, J. Zhang, *Angew. Chem. Int. Ed.* 2017, **56**, 6853-6858.

10. J. Ren, X. Sun, Y. Wang, R. Song, Z. Xie, S. Zhou, P. Chen, *Adv. Opt. Mater.* 2018, **6**, 1701273-1701280.

11. C. Zheng, L. Huang, Q. Guo, W. Chen, W. Li, H. Wang, *RSC Adv.* 2018, **8**, 10267-10276.

12. C. Zheng, L. Huang Q. Guo, W. Chen, W. Li, *Opt. Laser Technol.* 2018, **107**, 281-290.

13. X. Wang, L. Bai, L. Shen, B. Yao, H. Huang, Y. Liu, Y. Song, Z. Kang, *Opt. Mater.* 2019, **95**, 109216-109220.

14. P. Surendran, A. Lakshmanan, G. Vinitha, G. Ramalingam, P. Rameshkumar, *Luminescence*. 2019, **35***,* 196-202.

15. K. P. Praseetha, K. Chandrasekharan, V. Soney, *Opt. Laser Technol.* 2020, **130***,* 106367-106375.

16. W. K. Kipnusu, C. D. Buendía, M. F. Alonso, J. Lancis, G. M. Vega, *Part. Part. Syst. Charact.* 2020, **37**, 2000093-2000102.

17. S. Pandiyan, L. Arumugam, S. P. Srirengan, R. Pitchan, P. Sevugan, K. Kannan, G. Pitchan, T.

A. Hegde, V. Gandhirajan, *ACS Omega*. 2020, **5**, 30363-30372.

18. Y. Orooji, H. G. Gol, B. Jaleh, M. R. R. Vaziri, M. Eslamipanah, *Nanomaterials*. 2021, **11**, 737-752.